Ram Accelerator: A New Chemical Method for Accelerating Projectiles to Ultrahigh Velocities

A. Hertzberg,* A. P. Bruckner,† and D. W. Bogdanoff‡
University of Washington, Seattle, Washington

A new method for accelerating projectiles from velocities of ~0.7 km/s up to ~12 km/s using chemical energy is presented in this paper. The concept, called the "ram accelerator," is based on gasdynamic principles similar to those of an airbreathing ramjet but operates in a different manner. The projectile, which resembles the center body of a ramjet, travels through a tube filled with a premixed gaseous fuel and oxidizer mixture. The tube becomes the outer cowling of the ramjet, and the energy release process travels with the projectile. By tailoring the propellant mixture along the tube, a nearly constant acceleration can be achieved. In principle, the ram accelerator can be scaled for projectile masses ranging from grams to hundreds of kilograms and is capable of ballistic efficiencies as high as 30%. A straightforward, quasisteady, one-dimensional approach is used to model the acceleration process. The experimental facility developed to investigate the concept is described, and the results of recent experiments are presented. The velocity range of 690–1500 m/s has been explored in a 4.88-m long, 38-mm bore accelerator tube. Using methane, oxygen, and various diluents, accelerations of up to 16,000 *g* have been achieved with 75 gm projectiles and gas fill pressures of 20 atm. Proof of concept has been demonstrated, and agreement between theory and experiment has been found to be very good.

I. Introduction

THE barrier to accelerating a projectile to very high velocities by chemical energy is rooted in the limitations of the driver.[1] Once the projectile is accelerated to velocities beyond the initial acoustic velocity of the driver gas, the ballistic efficiency falls off very rapidly as the driving gas expends most of its energy in accelerating itself.[§] While several methods of achieving high acoustic velocities have been employed, such as precompression of the driver gas (two-stage gun), combustion heating, or electrical heating of a light driver gas, these methods result in relatively low ballistic efficiencies at high velocities and uneven acceleration profiles.[1]

Studies carried out by the authors since mid 1983 have led to a promising new technique called the "ram accelerator," by which relatively large masses (up to hundreds of kilograms) can, in principle, be accelerated efficiently to velocities up to 12 km/s by using chemical energy in a new manner. The basic principle involves an energy release process that travels with the projectile. Unlike a rocket, however, with this new concept there is no propellant on board the projectile. The ballistic efficiency remains high up to extremely high velocities and the acceleration can be maintained at a nearly constant level. While the gasdynamic principles of the ram accelerator are similar in many respects to those of the conventional airbreathing ramjet, the device is operated in a different manner.

Supersonic ramjets with subsonic combustion operate efficiently in the Mach number range of about 2–5.[2] Consider a conventional ramjet with an outer cowling and an internal body comprising a forward supersonic diffuser, a combustion section, and a convergent-divergent nozzle (Fig. 1). The performance of such a configuration flying through the atmosphere can be readily calculated. The fuel, however, must be carried on board, and the engine efficiency is limited by aerodynamic drag and by difficulties in obtaining high efficiency diffusers in the higher Mach number ranges. The thrust is limited by the density of the atmosphere, and the sound speed of the working gas is fixed by the temperature and composition of the atmosphere.

In the ram accelerator concept (Fig. 2), the internal body is a projectile fired into a tube and the cowling is now the wall of the tube. This affords the ability to control the pressure, composition, chemical energy density, and speed of sound (and, hence, Mach number) of the gas entering the ramjet engine. The gaseous propellant, consisting of premixed fuel and oxidizer, such as methane and oxygen or hydrogen and oxygen, fills the tube so that no fuel or oxidizer need be carried by the projectile. Since the fuel and oxidizer are premixed, the difficulties in obtaining rapid and complete mixing that are encountered in conventional subsonic combustion and supersonic combustion ramjets are circumvented.

The concept of flying a ramjet in a tube is not, in itself, new. For example, Wilbur et al., have proposed a direct space launch scheme involving electrical heating to accelerate payloads to 14-15 km/s.[3,4] However, the problems of electrical energy management and release for the required large payloads appear formidable. Slutsky and Tamagno proposed a supersonic combustion ramjet-in-tube concept in 1967,[5] and recently, Glasser suggested a ramjet-in-tube concept in which the projectile carries a solid fuel and the tube is filled with oxidizer.[6] However, neither of these two investigations has appeared in the open literature. Insofar as the authors know, none of these concepts has been explored experimentally.

Five modes of ram accelerator operation, which span the velocity range of 0.7-12 km/s, have been developed and studied by the authors. These concepts differ from the

Received Nov. 18, 1986; revision received June 5, 1987.

*Director, Professor of Aeronautics and Astronautics, Aerospace and Energetics Research Program. Fellow AIAA.

†Research Associate Professor of Aeronautics and Astronautics, Aerospace and Energetics Research Program. Member AIAA.

‡Research Engineer, Aerospace and Energetics Research Program. Member AIAA.

[§]Ballistic efficiency is defined here as the ratio of the rate of change of kinetic energy of the projectile to the rate of expenditure of chemical energy. This is an instantaneous efficiency that varies during the acceleration process. The overall ballistic efficiency is the ratio of the total change in kinetic energy of the projectile to the total chemical energy expended.

prior work noted previously in that the projectile flies through a premixed fuel-oxidizer mixture and uses energy release modes and configurations not heretofore considered. These include two subsonic combustion modes (one of which involves thermally choked combustion), a normal overdriven detonation mode, and two oblique detonation modes. The basic principles of all five acceleration modes are summarized in section II of this paper. The remainder of the paper deals with the thermally choked subsonic combustion mode. Details of the other modes are presented elsewhere.[7] In section III the analytical models used to date in the investigation of the thermally choked mode are discussed. The experimental facility constructed for proof-of-concept studies is described in section IV and the results of experiments spanning the velocity range 690-1500 m/s, using methane-based propellant mixtures, are presented in section V.

II. Ram Accelerator Drive Modes

The subsonic combustion ram accelerator drive modes are shown in Fig. 2. The projectile is injected into the accelerator tube at approximately 700 m/s by a conventional powder or gas gun. The gas mixture in the accelerator tube is chosen so that the projectile Mach number is initially in the range of 2.5–3. The cone angle of the nose is such that the oblique shock system in the diffuser does not initiate combustion. A normal shock is located downstream of the projectile throat; this shock is also not strong enough to initiate combustion. In the geometry of Fig. 2a, the combustion zone is at the projectile waist and is fully subsonic. A convergent-divergent nozzle serves to choke the exhaust gases mechanically and maintain the normal shock on the projectile. In the thermally choked case (Fig. 2b), the combustion zone is established behind the projectile, and the choking of the flow by the heat release stabilizes the normal shock on the projectile. In both cases combustion is initiated by either an onboard ignitor or an external ignitor mounted on the launch tube.

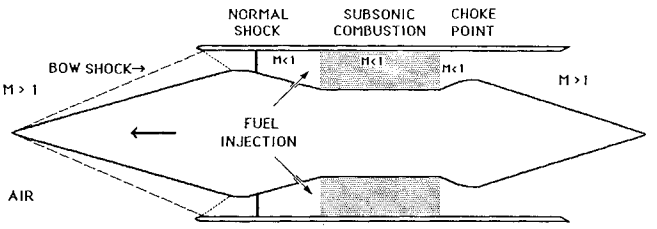

Fig. 1 Schematic of conventional supersonic airbreathing ramjet.

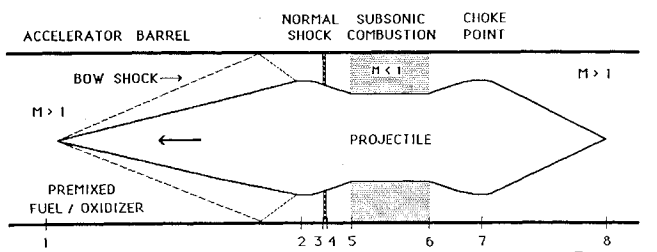

a) Mechanically choked mode.

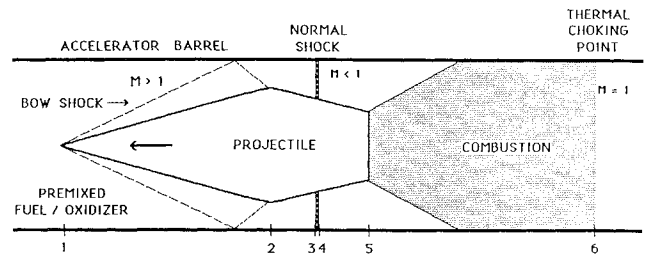

b) Thermally choked mode.

Fig. 2 Schematic of subsonic combustion ram accelerator concepts.

Above velocities of approximately 2.7–3 km/s subsonic combustion can no longer maintain a sufficiently high ballistic efficiency, even with hydrogen-based propellant mixtures. To continue efficient acceleration to higher velocities, three alternative concepts, which employ detonation waves to generate combustion, have been developed by the authors. These concepts are illustrated in Figs. 3 and 4. In all three cases, the projectile velocity must exceed the Chapman-Jouguet (C-J) detonation speed of the propellant gas. A transition to one of the detonation modes can be effected by having an abrupt change of propellant mixture in the accelerator tube at the appropriate location, using a thin diaphragm to separate the mixtures. If the second mixture is tailored to have a detonation speed sufficiently below the speed of the projectile, transition to one of the detonative modes occurs automatically; the specific mode depends on the projectile geometry.

Figure 3 shows the normal overdriven detonation wave mode of propulsion. The projectile Mach number is sufficiently high (typically greater than 6) for the normal shock to initiate combustion, which occurs in a very thin layer immediately behind the shock. The Mach number following heat release is subsonic, consequently the shock and reaction zone together constitute an overdriven detonation wave.[8]

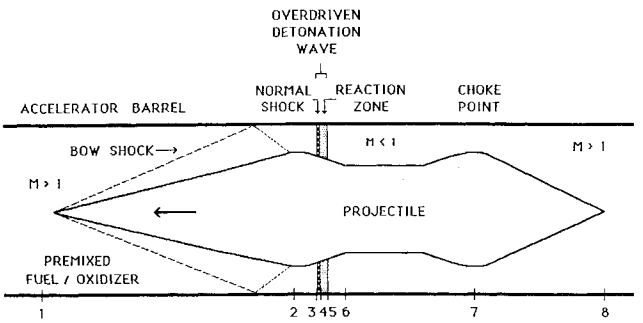

Fig. 3 Schematic of overdriven detonation ram accelerator concept.

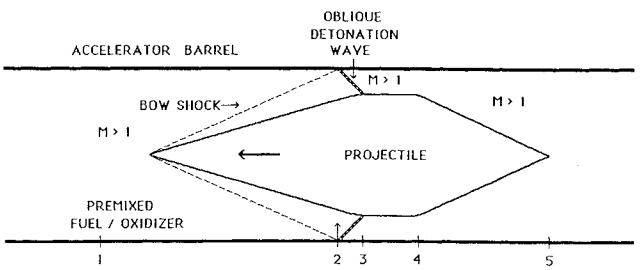

a) Type I oblique detonation mode.

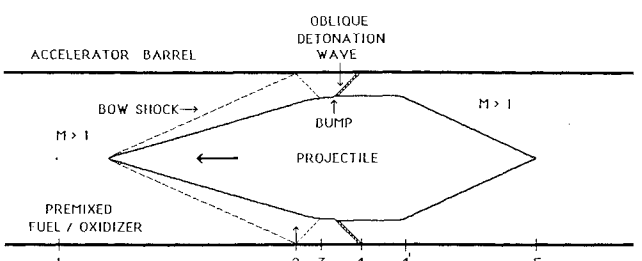

b) Type II oblique detonation mode.

Fig. 4 Schematic of oblique detonation ram accelerator concepts.

The choking of the flow in the exhaust nozzle keeps the detonation wave overdriven and the region of increasing flow area behind the diffuser throat stabilizes the wave. The projectile has a configuration similar to that of the subsonic combustion mode projectile of Fig. 2a. Consequently, a projectile of this geometry could first be accelerated by the subsonic combustion mode and then by the overdriven detonation mode. The maximum velocity capability of the overdriven detonation mode is ~5 km/s.

Figure 4 shows two oblique detonation drive concepts. In the Type I oblique detonation concept (Fig. 4a), the cone angle of the nose, the projectile velocity, and the speed of sound of the mixture are tuned so that the initial conical shock does not initiate combustion, but the reflected shock does. In operation, the reflected shock becomes an oblique detonation wave, which may be either C-J or overdriven. The projectile geometry is chosen so that the reflected detonation wave strikes the projectile just aft of the shoulder.

The Type II oblique detonation concept is shown in Fig. 4b. In this concept, the forward cone of the projectile is chosen so the combustion is not initiated by the compression process. Instead, a small squat frustum of a cone, with a relatively blunt cone angle, is inserted into the projectile profile to initiate an oblique detonation wave. This frustum or bump could be located anywhere along the cylindrical section of the projectile. In this oblique detonation mode, as well as in the Type I mode, the flow is supersonic throughout.

In principle, the oblique detonation ram accelerator modes can attain velocities up to 15 km/s. The propellant mixtures used at the higher velocities are 2 $H_2 + O_2$ plus He or excess H_2 diluent. Estimates of heat transfer rates to the projectile, however, indicate that intube aerodynamic heating and ablation become severe at velocities exceeding 6 km/s, depending on the specific propellant composition employed. In order to reduce the heat transfer to the projectile and extend the practical velocity limit, the authors have investigated a method of laying down a cylindrical core of pure hydrogen, surrounded by the propellant mixture.[7] This approach allows operation of the ram accelerator to velocities up to ~12 km/s.

The various modes of propulsion discussed above are scalable from fractions of a kilogram to hundreds of kilograms and can be patched together in appropriate combinations to span the entire velocity range from ~0.7 km/s to ~12 km/s. As noted earlier, the subsonic combustion projectile configuration of Fig. 2a can also be operated in the overdriven detonation mode (Fig. 3) to span the range of 0.7-5 km/s. The thermally choked projectile configuration (Fig. 2b) can be operated in the Type I or Type II oblique detonation modes (Fig. 4) to reach a velocity up to 12 km/s. Transition from the subsonic combustion modes to the detonation modes can be made at a velocity as low as ~2 km/s by judicious choice of a low detonation speed gas mixture.[8] In each mode the heat and pressure pulses travel with the projectile, distributing the heat over the entire length of the launch tube. Consequently, the temperature rise of the tube is relatively small and very little tube wear is expected.

For the ram accelerator, specific impluse does not have its usual meaning because no fuel or oxidizer is carried onboard the projectile. Rather, the performance of the device can be characterized by two main parameters: thrust pressure ratio and ballistic efficiency. The thrust pressure ratio is the net average drive pressure on the projectile (the thrust divided by the maximum projectile cross-sectional area) divided by the maximum cycle pressure. This ratio is an important performance parameter because it provides a measure of the device's launch capability vs the maximum pressure the projectile and launch tube must survive. The thrust pressure ratios of the ram accelerator modes are in the range of ~0.15-0.7 for the subsonic combustion modes and ~0.15-0.4 for the detonation modes.[7] Ballistic efficiencies of 15-30% are realizable with all five acceleration modes. For comparison, the overall ballistic efficiency of a two-stage light gas gun is typically less than 10% at 3 km/s and less than 3% at 8 km/s.[9]

III. Analysis of Thermally Choked Subsonic Combustion Mode

Simplified 1-D Analysis

The thermally choked subsonic combustion mode can be modeled in a particularly straightforward manner that illustrates the fundamental characteristics of this mode of propulsion. This simplified approach is one-dimensional, quasi-steady and inviscid. The conservation equations are applied to the control volume between stations 1 and 6 in Fig. 2b, without including any of the details of the flow, such as the oblique and normal shocks, subsonic diffusion, base recirculation zone, and combustion shear layer. In addition, friction on the tube walls and projectile body is neglected. The ideal gas equation of state is used with one set of values for the molecular weight and specific heat ratio before combustion and a second set after combustion. This simplified approach offers a good overall approximation of the performance characteristics of the thermally choked mode of propulsion and is useful for evaluating the suitability of various propellant mixtures over velocity ranges of interest.

The conservation equations are applied in the frame of reference of a stationary projectile. Consequently, the tube wall moves relative to the projectile with the same velocity as the gas upstream of the projectile. The upstream boundary of the control volume (station 1) is located just forward of the projectile nose tip, and the downstream boundary (station 6) coincides with the plane where thermal choking occurs. Application of the momentum and continuity equations to the control volume results in the following relation for the nondimensional thrust on the projectile:

$$\frac{F}{p_1 A} = \frac{p_6}{p_1}(1+\gamma_6) - (1+\gamma_1 M_1^2) \tag{1}$$

where F is the thrust, A is the tube cross-sectional area, p_1 and p_6 are the static pressures entering and leaving the control volume, γ_1 and γ_6 are the specific heat ratios before and after combustion and M_1 is the Mach number of the flow entering the control volume. Note that at the thermal choking point $M_6 = 1$.

From continuity and the ideal gas law it can be shown that

$$\frac{p_6}{p_1} = M_1 \left[\left(\frac{T_6}{T_1} \right) \left(\frac{\gamma_1 m_1}{\gamma_6 m_6} \right) \right]^{1/2} \tag{2}$$

where T_1 and T_6 are the static temperatures at stations 1 and 6 and m_1 and m_6 are the respective molecular weights. Using the isentropic relations at stations 1 and 6, the temperature ratio T_6/T_1 can be expressed as follows:

$$\frac{T_6}{T_1} = \frac{T_{t_6}}{T_{t_1}} \left[\frac{2 + (\gamma_1 - 1) M_1^2}{\gamma_6 + 1} \right] \tag{3}$$

where the subscript t denotes stagnation conditions. The ratio T_{t_6}/T_{t_1} is obtained from application of the energy equation across the control volume:

$$\frac{T_{t_6}}{T_{t_1}} = \frac{C_{p_1}}{C_{p_6}} \left(1 + \frac{\Delta q}{C_{p_1} T_{t_1}} \right) \tag{4}$$

where C_{p_1} and C_{p_6} are the specific heats at constant pressure before and after combustion, respectively. The parameter Δq is the heat of reaction of the propellant gas mixtures and,

together with the values of γ_1, γ_6, C_{p_1}, and C_{p_6}, is obtained from a separate equilibrium combustion computation similar to that of Barrére.[10] The initial conditions for combustion are approximated as those behind a normal shock with a pressure ratio of 20. Substituting Eqs. 2-4 into Eq. 1 yields

$$\frac{F}{p_1 A}=\frac{\gamma_1 M_1}{\gamma_6}\left\{2\left(\frac{\gamma_6^2-1}{\gamma_1-1}\right)\left[1+\frac{\gamma_1-1}{2}M_1^2+\frac{\Delta q}{C_{p_1}T_1}\right]\right\}^{1/2}-(1+\gamma_1 M_1^2) \tag{5}$$

It can be seen that the thrust, F, is directly proportional to the initial propellant fill pressure, p_1. Combining Eq. 5 with the equation of motion,

$$\frac{dU_1}{dx}=\frac{F}{mU_1} \tag{6}$$

and integrating yields the velocity, U_1, of the projectile of mass m as a function of position, x, along the launch tube.

As the projectile accelerates, M_1 increases and the thrust decreases, reaching zero at a flight Mach number given by

$$M_1=[(\alpha+\sqrt{\alpha^2-\beta})/\beta]^{1/2} \tag{7}$$

where

$$\alpha=\left(\frac{\gamma_1}{\gamma_6}\right)^2\left(\frac{\gamma_6^2-1}{\gamma_1-1}\right)\left(1+\frac{\Delta q}{C_{p_1}T_1}\right)-\gamma_1$$

and

$$\beta=(\gamma_1/\gamma_6)^2$$

It can be readily shown that this result corresponds to the Mach number of a one-dimensional C-J detonation wave propagating in the same gas mixture.[8] Thus, in the absence of friction, the limiting velocity of the thermally choked mode of propulsion is the C-J detonation velocity.

The maximum thrust occurs at

$$M_1=\left[\left(\frac{\gamma_6-1}{\gamma_1-1}\right)\left(1+\frac{\Delta q}{C_{p_1}T_1}\right)\right]^{1/2} \tag{8}$$

Interestingly, this corresponds to the condition $U_6=U_1$, where U_1 and U_6 are the flow velocities entering and leaving the control volume, i.e., the thrust is maximum when the thermal choking point is stationary with respect to the launch tube. Substitution of Eq. (8) in Eq. (5) yields the following expression for the maximum thrust:

$$\left(\frac{F}{p_1 A}\right)_{\max}=\frac{\gamma_1(\gamma_6-1)}{\gamma_6(\gamma_1-1)}\left(1+\frac{\Delta q}{C_{p_1}T_1}\right)-1 \tag{9}$$

For the special case of constant γ and C_p, the maximum thrust is directly proportional to the heat of reaction, i.e.,

$$\left(\frac{F}{p_1 A}\right)_{\max}=\frac{\Delta q}{C_p T_1} \tag{10}$$

As noted earlier, the ballistic efficiency, η, is defined as the rate of change of projectile kinetic energy divided by the rate of heat addition to the flow, i.e.,

$$\eta=\frac{FU_1}{\dot{m}\Delta q} \tag{11}$$

where $\dot{m}=\rho_1 U_1 A$ is the mass flow rate through the control volume. Using continuity, the ideal gas law, and the definition of the speed of sound, $a_1=\sqrt{\gamma_1 R_1 T_1}$, it can be shown that

$$\eta=\left(\frac{F}{p_1 A_1}\right)\frac{a_1^2}{\gamma_1 \Delta q} \tag{12}$$

Thus, for a given propellant mixture, the ballistic efficiency is directly proportional to the nondimensional thrust. It follows that the ballistic efficiency reaches its maximum at the maximum thrust condition and goes to zero as the projectile velocity approaches the C-J detonation velocity. It is interesting to note that for the special case of constant γ and C_p, the maximum value of the ballistic efficiency is

$$\eta_{\max}=(\gamma-1)/\gamma \tag{13}$$

This sets an upper limit to the ballistic efficiency in the range of ~0.16-0.30 for propellant mixtures of interest, depending on the effective average value of γ.

Clearly, the key to optimum performance is to keep the projectile Mach number within a narrow range close to that corresponding to the peak thrust and efficiency. This can be accomplished by having a graded propellant mixture with a speed of sound that increases toward the muzzle of the launch tube, or by dividing the launch tube into several segments filled with different propellant mixtures and constraining the projectile to operate in a limited Mach number range in each segment.

This simple model does not predict the lower operational limit of the device because there is no specification of the projectile diameter and hence of the diffuser area ratio. It is this ratio, the oblique shock entropy losses, and the heat release Δq, that define the minimum value of M_1 at which the diffuser can "start."

More Detailed 1-D Analysis

The more detailed analytic approach used in the investigation of the subsonic combustion modes includes some of the major details of the flow around the projectile. This analysis is also quasisteady, inviscid, and one-dimensional, except for the oblique shock waves. The flow is considered isentropic except for the normal and oblique shocks and the combustion. Figure 2b illustrates the principal features of the model. Although the flowfield generated by the conical bow shock can be readily computed,[11] the multiple shock reflections from the tube wall and projectile body in the nonuniform flow are not analytically tractable. This problem is best solved by CFD methods.[12] For the purposes of the present approach the supersonic portion of the diffuser has been approximated by an equivalent 2-D wedge diffuser with one reflected shock. The validity of this simplifying assumption is borne out by the fact that the performance of the device is insensitive to the efficiency of the supersonic portion of the diffuser.

The normal shock stands behind the diffuser throat in the diverging portion of the flow, at a location governed by the projectile Mach number and the heat release in the combustion zone. The shock jump conditions are treated by standard techniques[13] and the shock is allowed to move in response to changing projectile velocity. The flow between the shock and the combustion zone is assumed isentropic, i.e., it is assumed that there is full pressure recovery at the projectile base prior to combustion. It is also assumed, for simplicity, that combustion occurs in the full tube area beginning just beyond the base of the projectile. The heat release process between stations 5 and 6 is treated by a conventional constant-area heat addition analysis coupled to an equilibrium chemistry combustion routine.[10] The details of the recirculation zone at the projectile base and the expanding shear layer between the combusting gases and the tube

wall are not considered. Also, the length of the combustion zone is not computed because no kinetics are included. The frictional drag on the projectile is computed separately, using the velocity field obtained from the inviscid analysis. The skin friction coefficient is assumed to be 0.003 in subsonic flow and is corrrected for Mach number effects in supersonic flow.[14]

In the absence of friction, both analytical approaches yield the same result, i.e., the variation of nondimensional thrust and ballistic efficiency with Mach number is the same in both cases for the same set of operational parameters. In the more detailed model the upper Mach number limit corresponds to the normal shock moving off the projectile. Since the base area of the projectile is finite, this condition occurs at a lower Mach number than the C-J detonation condition and is governed by the ratio of base area to tube cross-sectional area. In addition, the second approach predicts a lower limit to the projectile Mach number, at which the normal shock stands just at the diffuser throat. This lower limit is a function of the ratio of the diffuser throat area to the tube cross-sectional area and Δq, the heat of combustion. For projectile geometries and propellant mixtures of interest, this Mach number is in the range of approximately 2.3–2.5. For some propellant mixtures of interest, however, Eq. (8) predicts that the maximum thrust occurs at a Mach number somewhat below the minimum defined previously. In those cases, therefore, the minimum starting Mach number defines the maximum attainable thrust condition.

As defined earlier, the thrust pressure ratio is the ratio of the average drive pressure on the projectile to the maximum pressure in the cycle. For the thermally choked mode the thrust pressure ratio, ϕ, is

$$\phi = \frac{F}{A_p p_5} = \left(\frac{F}{p_1 A}\right)\left(\frac{p_1}{p_5}\right)\left(\frac{A}{A_p}\right) \tag{14}$$

where A_p is the maximum projectile cross-section area and p_5 is the maximum static pressure, which occurs at station 5, the projectile base. Because p_5 is a monotonically increasing function of the projectile Mach number, the maximum thrust pressure ratio occurs at a lower Mach number than the maximum thrust; however, it goes to zero at the same Mach number as the thrust, i.e., the C-J detonation condition. A high value of ϕ is desirable because it permits a higher fill pressure (hence higher thrust and acceleration) to be used for a given launch tube wall strength.

IV. Experimental Ram Accelerator Facility

The principal components of the University of Washington ram accelerator facility are a single-stage light gas gun, a ram accelerator section, a final dump tank, and a projectile decelerator. Associated subsystems are the gas handling system, instrumentation, and data acquisition system.

The 38 mm bore single-stage light gas gun is of conventional design[1] and is capable of accelerating the sabot/projectile combination (typical combined mass $\approx$100 g) to speeds up to approximately 1200 m/s. The muzzle of the gun is connected to a perforated wall tube that passes through an evacuated tank that serves as a dump for the helium driver gas.

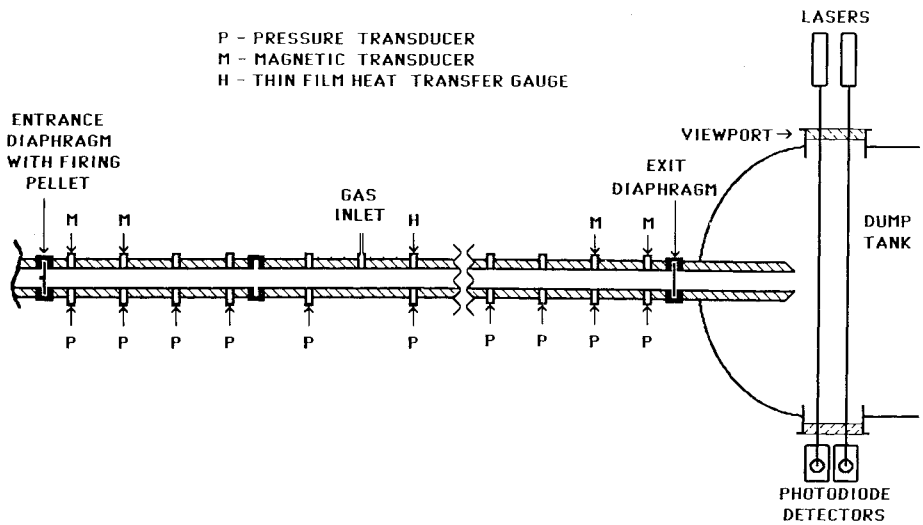

Fig. 5 Schematic of ram accelerator test section and associated instrumentation.

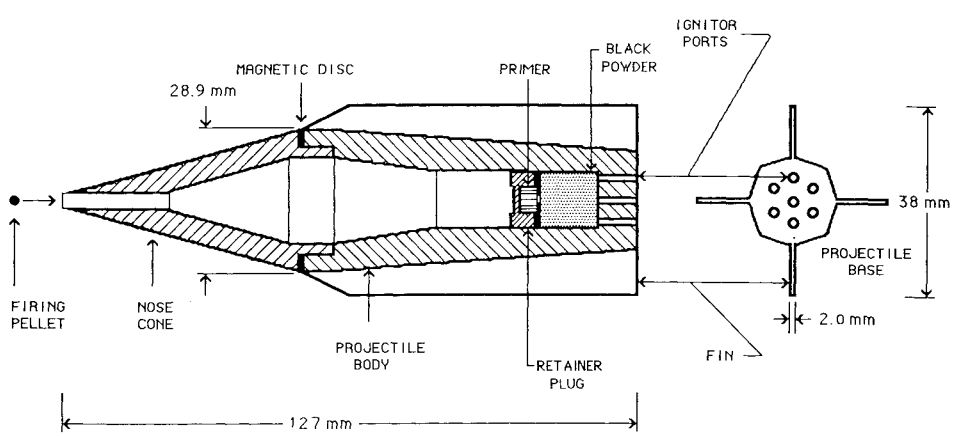

Fig. 6 Cross-section of experimental ram accelerator projectile.

The ram accelerator section (Fig. 5) consists of three steel tubes with an I.D. of 38 mm and a total length of 4.88 m. There are a total of 12 pairs of diametrically opposed instrumentation ports disposed at regular intervals along the tube. A Kistler pressure transducer is located at each of the 12 observation stations. The remaining ports are used to mount electromagnetic coil velocity transducers, heat transfer gages, and light fiber probes. A 16-channel, 1 MHz digital data acquisition system (DAS) is used to process the data.

The ram accelerator section is designed to operate at propellant fill pressures up to 50 atm. Thin Mylar diaphragms close off each end. The fuel, oxidizer, and diluent gases are metered using sonic orifices, sent to a gas mixer (carburetor) and then on to the ram accelerator section.

When the projectile leaves the ram accelerator section it travels through a 76-cm-long drift tube and then across the final evacuated dump tank, where it flies free. The tank has a pair of 25-cm-diameter viewing ports for spark photography. A two-beam laser velocity measuring system (Fig. 5) permits a final measurement of the velocity of the projectile. The projectile is brought to a stop in steel lathe turnings in a large-diameter decelerator tube.

Projectile Configuration

The projectile geometry currently in use in the experimental studies is illustrated in Fig. 6. It is fabricated from magnesium in two pieces: the nose cone and the body with integral fins. The purpose of the fins is only to center the projectile in the tube. At the threaded joint between the nose and body is sandwiched a thin sheet of flexible magnetic material which interacts with the electromagnetic transducers to provide velocity data independent of the exact disposition of pressure waves on the projectile. The length of the projectile is 12.7 cm and its maximum diameter is 28.9 mm which results in a diffuser area ratio of 2.37. The all-up mass of the projectile is 75 gm and that of the Lexan launching sabot is 23 gm.

The projectile carries within it an ignitor consisting of a pistol primer and a charge of 0.5 gm of black powder. Upon entering the ram accelerator section, the projectile pierces the upstream Mylar diaphragm to whose center is affixed a small metal pellet. The pellet is scooped up by the projectile in flight and dimples a thin aluminum shield which fires the pistol primer. The hot gases generated by the powder charge exit through seven exhaust ports at the base of the projectile and enter the recirculation region behind the projectile, igniting the combustible gas. Ignition delay is less than 0.5 ms and the duration of the powder burn is 2-3 ms. The truncated base of the projectile acts as a flame-holding dump combustor for the thermally choked mode of operation.

V. Results and Discussion

The experiments to date have been carried out using methane and oxygen as the fuel and oxidizer, and carbon dioxide, nitrogen, and excess methane as the diluents. The mixture used in the lower velocity range (690-1260 m/s) has been $CH_4 + 2O_2 + 6CO_2$. To explore higher velocity ranges (1000-1500 m/s) a mixture of $2.5CH_4 + 2O_2 + XN_2$ has been used, where X has been varied between 5 and 6. The use of CO_2, N_2, and excess CH_4 as diluents serves two purposes: it tailors the speed of sound of the mixtures so that the initial projectile Mach number exceeds the minimum required to start the diffuser, and it minimizes the possibility of the combustion wave developing into a detonation. Propellant fill pressures of 3-20 atm absolute and injection velocities in the range of 680-1200 m/s have been investigated in numerous test firings.

A pair of electromagnetic and pressure transducer outputs obtained at a distance of 1.51 m from the entrance diaphragm for a test run in $2.5\ CH_4 + 2\ O_2 + 6\ N_2$ at 20 atm

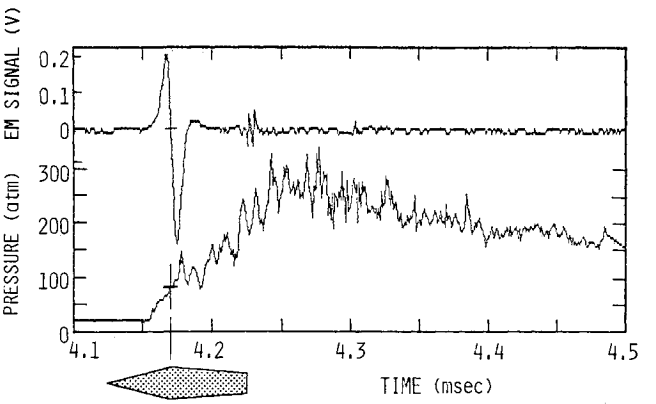

Fig. 7 Electromagnetic (EM) and pressure transducer signals in ram accelerator. Propellant mixture: $2.5\ CH_4 + 2\ O_2 + 6\ N_2$; $p_1 = 20$ atm; $x = 1.51$ m; $U_1 = 1300$ m/s.

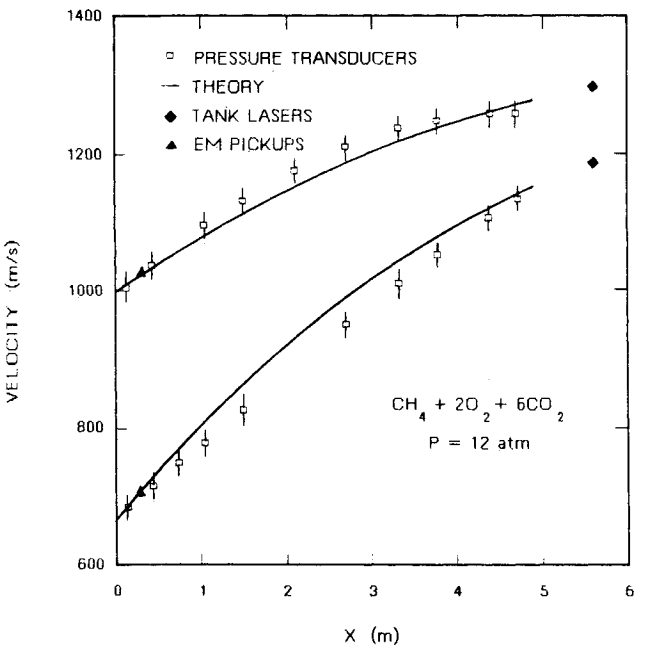

Fig. 8 Comparison of experimental and theoretical velocity profiles in ram accelerator for $CH_4 + 2O_2 + 6CO_2$ propellant mixture and initial velocities of 690 and 1000 m/s. Projectile mass = 75 g.

is shown in Fig. 7. The projectile velocity is 1300 m/s and the Mach number is 3.62. Time is measured from the instant of DAS triggering, and pressure is displayed in atmospheres. The pressure trace first exhibits a small but distinct pressure pulse, which is generated by the oblique shock system in the projectile's diffuser section. A series of pulses follows that increases the pressure to a peak of ~280 atm, after which the pressure decays. The increase in pressure after the initial oblique shocks represents the normal shock, which appears to consist of a complex system of oblique and normal shocks similar to that observed in supersonic flows in long ducts.[13] The decay in pressure following the peak is due to the heat addition choking the flow and the subsequent expansion of the combustion products into the tube behind the choking point. The pressure signatures and preliminary thin film heat transfer gage data indicate that the combustion zone extends about 5-15 tube diameters behind the projectile, depending on the propellant mixture and the initial fill pressure.

Once combustion is established, the peak pressure of the cycle is observed to fluctuate about an approximately cons-

tant mean value throughout the acceleration process. The measured ratio of mean peak pressure to tube fill pressure is ~15 for the N_2 diluted mixture and ~18 for the CO_2 diluted mixture. The experimental pressure signatures are similar in shape and the pressure ratios are similar in magnitude at all the fill pressures examined to date (3–20 atm) for the respective propellant mixtures.

The upper trace in Fig. 7 displays the output of an electromagnetic transducer mounted at the same axial station as the pressure transducer. The zero crossing point of the electromagnetic signal corresponds to the time of arrival of the projectile's magnetic disk. Since this disk is at the projectile

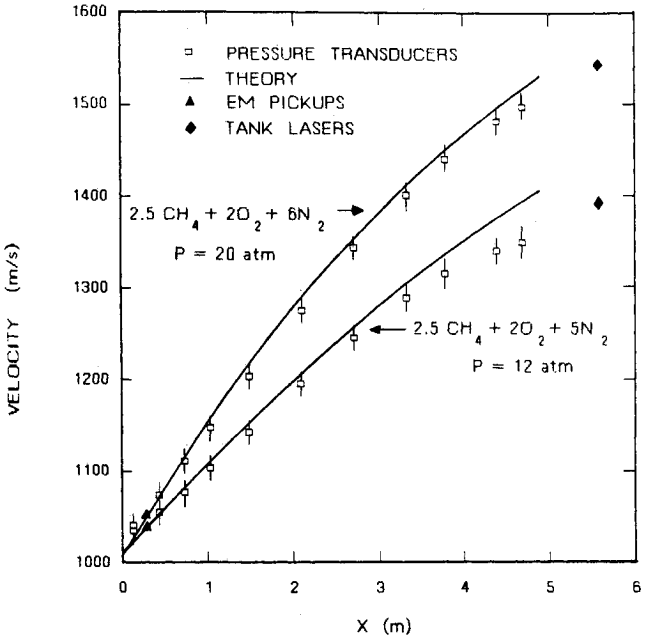

Fig. 9 Comparison of experimental and theoretical velocity profiles in ram accelerator for $2.5CH_4+2O_2+5N_2$ propellant mixture at 12 atm and $2.5CH_4+2O_2+6N_2$ propellant mixture at 20 atm. Initial velocity = 1020 m/s; projectile mass = 75 g.

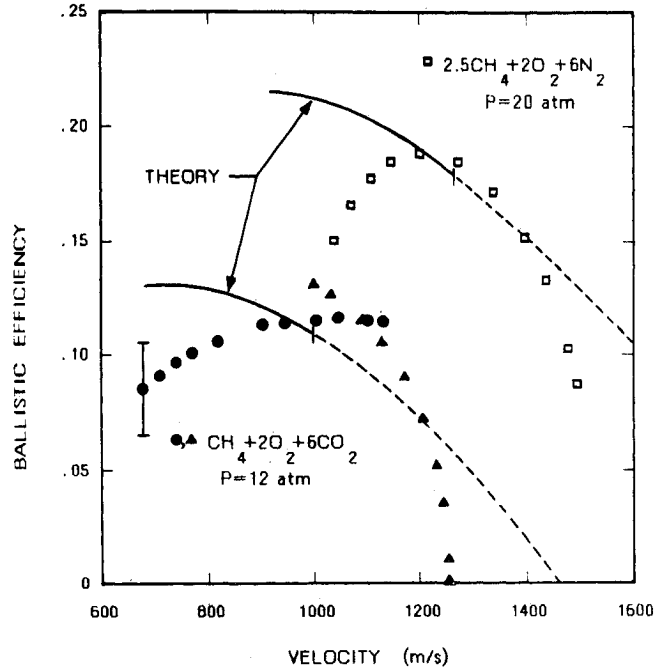

Fig. 10 Ballistic efficiency as a function of projectile velocity for $CH_4+2O_2+6O_2$ and $2.5CH_4+2O_2+6N_2$ propellant mixtures. Typical error bar shown on leftmost data point.

throat, the location of the shock system on the projectile relative to the throat can be determined. A profile of the projectile scaled to the local velocity is shown under the pressure trace in Fig. 7 to illustrate this point. It can be seen that the pressure reaches its maximum somewhat behind the projectile, however, it is likely that this higher pressure is communicated to the projectile through the subsonic recirculation region behind the base of the projectile.

The velocity of the projectile is deduced from the distance-time history of its bow shock. The x-t plot is curve fit with a fourth-order polynomial, and velocities are obtained by differentiation. Representative results from experiments performed at 12 atm using the $CH_4+2\ O_2+6\ CO_2$ propellant mixture and two different entrance velocities, 690 m/s ($M_1=2.36$) and 1000 m/s ($M_1=3.42$) are shown in Fig. 8. Results for two slightly different nitrogen diluted mixtures at pressures of 12 and 20 atm respectively and an entrance velocity of 1020 m/s ($M_1=2.84$) are shown in Fig. 9. The plotted points represent the experimental data obtained from the pressure signatures, and the curves represent the velocity profiles predicted by the quasisteady one-dimensional model, with friction included. (Not all the pressure transducers of the complement of twelve were operative at the time the experiments were performed.) The figures also display the independent velocity measurements obtained with the electromagnetic transducers and the laser. A projectile velocity of 1500 m/s and a peak acceleration of 16,000 g have been obtained in the ram accelerator tube using the $2.5\ CH_4+2\ O_2+6\ N_2$ mixture at 20 atm fill pressure.

The two N_2 diluted cases shown in Fig 9 display an ignition delay that occupies about the first half meter of the test section. Since the quasisteady analytical model does not treat transient phenomena, the theoretical curves in these cases were matched to the first experimental points at which full drive was established. In the remaining cases the ignition transient was very rapid and full drive was almost immediately established. The minimum entrance velocity required with the "slow" mixture (i.e, the one using CO_2 as the diluent) is ~690 m/s ($M_1=2.36$). Below that velocity an unstart condition results because the diffuser area ratio is too large for the corresponding Mach number.[13] The "fast" mixtures (using N_2 and excess CH_4 as diluents) require a minimum entrance velocity of ~850 m/s ($M_1=2.37$).

It has been observed that additional acceleration occurs in the short evacuated drift tube that follows the ram accelerator. This is shown by the solid, diamond-shaped points plotted to the right of the curves in Figs. 8 and 9. These correspond to the projectile velocity at the end of the drift tube, as measured by the two-beam laser system. The velocity increment ranges from ~20 m/s to ~40 m/s, depending on the fill pressure and the velocity range. This acceleration is due to the net forward thrust generated by the high pressure gas that follows the projectile as it exits the ram accelerator tube. Separate investigations of this phenomenon have shown that the bulk of the additional impulse is imparted to the projectile within about 20 tube diameters of the exit diaphragm.

Figures 10 and 11 show plots of the ballistic efficiency and thrust pressure ratio as functions of projectile velocity for the $CH_4+2\ O_2+6\ CO_2$ and $2.5\ CH_4+2\ O_2+6\ N_2$ propellant mixtures. The solid/dashed curves represent the theory and the plotted points, the results for the experiments shown in Figs. 8 and 9. The transition from solid to dashed line on the theoretical curves represents the point where theory predicts the normal shock falls off the base of the projectile. The dashed portion of the curves indicates the performance predicted for a projectile whose rear body tapers down to a point. On such a projectile the normal shock would, in principle, stay on the body at velocities up to the C-J detonation speed, as discussed earlier.

The ballistic efficiency, η, is computed by means of Eq. (12). The value of Δq is obtained from the theoretical com-

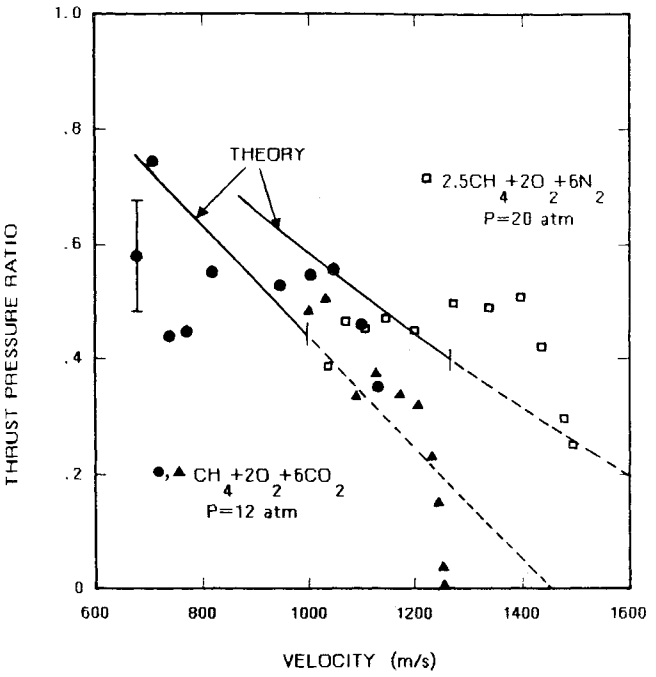

Fig. 11 Thrust pressure ratio as a function of projectile velocity for $CH_4+2O_2+6O_2$ and $2.5CH_4+2O_2+6N_2$ propellant mixtures. Typical error bar shown on leftmost data point.

bustion calculations and the thrust, F, is obtained from the second derivative of the projectile's x-t history and Newton's law of motion $F=ma$, where a is the acceleration. This procedure tends to amplify small errors in time measurements and imperfections in the x-t curve fit to the data, resulting in relatively large error margins. The magnitudes of the experimental data points are in reasonable agreement with the theoretically predicted values for each propellant mixture, except at the lowest and highest velocities. At the low velocity end, ignition delays and starting transients probably account for much of the observed discrepancy. At the high velocity end, it can be seen that the ballistic efficiency goes to zero at a lower velocity than the C-J detonation velocity but at a higher velocity than predicted for the finite base area of the projectile. This is probably a result of the complex normal shock system falling off the rear of the projectile in a gradual manner, rather than abruptly, as the Mach number increases. In experiments to date, velocities of the order of ~80–85% of the C-J detonation speed have been consistently attained.

It should be noted that the ballistic efficiency (both theoretical and experimental) of the N_2 diluted mixture is significantly higher than that of the CO_2 diluted mixture even though Δq is approximately the same for both mixtures. The peak values predicted by the theory [Eqs. (12) and (9)] are ~21% and ~13% respectively, and the experimental maxima are ~19% and ~13% respectively. The experimental maxima do not occur at the predicted velocities because of the effect of the starting transients. The higher performance of the N_2 diluted mixture stems partly from a somewhat higher nondimensional thrust, but primarily from its higher speed of sound, on which the ballistic efficiency depends quadratically [see Eq. (12)].

The thrust pressure ratio, ϕ, (Fig. 11) is computed from Eq. (14) using the thrust and peak pressure data. The experimentally determined values of ϕ thus have a relatively large uncertainty and significant scatter due to the inherent uncertainty in the values of F noted earlier and the difficulty in accurately determining the peaks of the pressure traces. The difficulty in obtaining accurate pressure data stems from the relatively noisy pressure signatures (see Fig. 7). This noise is a result of complex wave interactions and transducer and tube wall resonances. Nevertheless, the trend of the experimental data is clear: the thrust pressure ratio has approximately the expected magnitude at a given velocity and decreases with increasing velocity. At the high velocity end for each propellant mixture the experimental thrust pressure ratio decreases rapidly as a result of the normal shock system falling completely off the rear of the projectile. This result is consistent with the rapid decrease in ballistic efficiency observed at similar velocities.

The attainment of velocity increments, ballistic efficiencies, and thrust pressure ratios consistent with theoretical predictions has established the proof of the thermally choked, subsonic combustion ram accelerator principle. The overall agreement between theory and experiment is very good, considering the simplicity of the models used, and indicates that the actual details of the flowfield and combustion are not critical to the overall performance of the device. Additional details on gasdynamic phenomena associated with this mode of propulsion are found in Ref. 15.

At the time the experiments presented here were performed, the attainable velocity increment was constrained by the propellant fill pressure and the length of the ram accelerator tube. Increasing the pressure and lengthening the tube will result in larger velocity increments. At the time of writing, the length of the test section was being increased to 12.2 m and the gas handling system was modified to permit propellant fill pressures up to 50 atm. The aim of these modifications is to achieve a velocity of 2500 m/s or greater and to permit the investigation of the detonation modes of propulsion.

VI. Conclusions

The ram accelerator principle is a promising and efficient concept for accelerating projectiles from velocities of ~0.7 km/s to as high as ~12 km/s using chemical energy. Several different modes of ram accelerator propulsion, which in principle span this velocity range, have been presented. Of these modes, the thermally choked, subsonic combustion mode has been discussed in detail. Experimental investigations over the velocity range of 690-1500 m/s, using methane-based propellant mixtures, have established the proof-of-principle of this mode of propulsion and are in good agreement with theoretical predictions. Ongoing investigations at the University of Washington are aimed at further developing the concept and demonstrating the detonation modes of acceleration.

Acknowledgments

This work was supported in part by USAF Contract F08635-84-K-0143. The authors are deeply indebted to their students, Carl Knowlen, Ivan Stonich, Dean Brackett, Dale Barr, Carl Engelbrecht, and Keith McFall, whose enthusiasm and diligence ensured the success of the project. Although it is not possible to acknowledge all of the colleagues with whom they had helpful discussions, the authors are particularly indebted to Ed Kepler of the United Technologies Research Center, East Hartford, Connecticut, for his invaluable discussions on the technology of ramjets, to Roger Strehlow of the University of Illinois, Urbana, Illinois, for his useful comments on the combustion and detonation aspects of this work, and to Hal Swift, President of Physics Applications, Inc., Dayton, Ohio, whose firm fabricated many of the components for the facility, for his useful suggestions about the mechanical and gasdynamic operating procedures employed. The authors are grateful also to the Kistler Instrument Corporation for its generous gift of the pressure transducers and related instrumentation, which have proved invaluable in the experimental investigations.

References

[1]Seigel, A. E., "Theory of High-Muzzle-Velocity Guns," *Interior Ballistics of Guns*, Krier, H. and Summerfield, M., eds., *Progress in Astronautics and Aeronautics*, Vol. 66, American Institute of Aeronautics and Astronautics, New York, 1979, pp. 135–175.

[2]Dugger, G. L., ed., *Ramjets*, AIAA Selected Reprint Series, American Institute of Aeronautics and Astronautics, New York, Vol. VI, 1969.

[3]Wilbur, P. J., Mitchell, C. E., and Shaw, B. D., "The Electrothermal Ramjet," *Journal of Spacecraft and Rockets*, Vol. 20, Nov.–Dec. 1983, pp. 603–610.

[4]Shaw, B. D., Mitchell, C. E., and Wilbur, P. J., "The Annular Flow, Electrothermal Plug Ramjet," *Journal of Propulsion and Power*, Vol. 1, Nov.–Dec. 1985, pp. 417–425.

[5]Slutsky, S. and Tamagno, J., General Applied Science Laboratories, Inc., Westbury, NY, 1967. Private communication by C. E. Kepler, United Technologies Research Center, East Hartford, CT, 1985.

[6]Glasser, A., Drexel University, Philadelphia, PA, private communication, 1984.

[7]Knowlen, C., Bruckner, A. P., Bogdanoff, D. W., and Hertzberg, A., "Performance Capabilities of the Ram Accelerator," AIAA Paper 87-2152, June 1987.

[8]Strehlow, R. A., *Fundamentals of Combustion*, R. E. Krieger Co., Malabar, FL, 1983, Ch. 9.

[9]H. F. Swift, Physics Applications, Inc., Dayton, OH, private communication, 1986.

[10]Barrére, M. et al., *Rocket Propulsion*, Elsevier, Amsterdam, 1960, pp. 142–149.

[11]Taylor, G. I. and Macoll, J. W., "The Air Pressure on a Cone Moving at High Speeds," *Proceedings of the Royal Society of London A*, Vol. 139, 1933, pp. 278–311.

[12]Bogdanoff, D. W. and Brackett, D. C., "A Computational Fluid Dynamics Code for the Investigation of Ramjet-in-Tube Concepts," AIAA Paper 87-1978, AIAA/SAE/ASME/ASEE 23rd Joint Propulsion Conference, San Diego, CA, June 29–July 2, 1987.

[13]Shapiro, A. H., *The Dynamics and Thermodynamics of Compressible Fluid Flows*, Vol. I, Ronald Press, NY, 1953, Chs. 4, 5, and 7.

[14]Schlichting, H., *Boundary Layer Theory*, 7th ed., McGraw-Hill, NY, 1979, pp. 715–718.

[15]Bruckner, A. P., Bogdanoff, D. W., Knowlen, C., and Hertzberg, A., "Investigation of Gasdynamic Phenomena Associated with the Ram Accelerator Concept," AIAA Paper 87-1327, June 1987.